XLVI CILAMCE
VITÓRIA - ES - BRAZIL - 2025
XLVI IBERO-LATIN AMERICAN CONGRESS ON COMPUTATIONAL METHODS IN ENGENEERING

A micromechanics-based approach to damage propagation in fiber-reinforced fractured cementitious materials

Marcos B. Guimarães[1], Cássio B. Aguiar[2], Samir Maghous[1]

[1]*Graduate Program in Civil Engineering, Federal University of Rio Grande do Sul*
Av. Osvaldo Aranha, 99, Porto Alegre/RS, Brazil
bressan.marcos@hotmail.com, samir.maghous@ufrgs.br
[2]*Department of Civil Engineering, Federal Technological University of Paraná*
R. Marcílio Dias, 635, Apucarana/PR, Brazil
cassio.barros.aguiar@gmail.com

Abstract. A model combining micromechanical reasoning with macroscopic thermodynamic concepts is formulated in this paper to evaluate the damage propagation in fiber-reinforced fractured cementitious materials. Unlike cracks, fractures are discontinuities able to transfer stress and can be regarded from a mechanical viewpoint as interfaces endowed with a specific behavior under normal and shear loading. Fibers are increasingly incorporated into cementitious materials to enhance their mechanical performance, durability, and ability to minimize the emergence and propagation of microfractures. Making use of the Mori-Tanaka homogenization scheme, this work employs a micromechanical approach based on Eshelby's equivalent inclusion theory to formulate the homogenized elastic behavior of fiber-reinforced fractured cementitious materials. In this context, fractures and fibers are modeled as oblate and prolate spheroids endowed with appropriate elastic properties. The proposed macroscopic damage model, reflecting fracture propagation at the microscopic scale, combines the above results with classical thermodynamic principles within the framework of damage mechanics, where the fracture density parameter is treated as a damage parameter at the macroscopic scale. The model's ability to capture damage-induced anisotropy is demonstrated through a comparison with experimental data on randomly distributed steel fiber-reinforced concrete, showing an accurate prediction of their strain-hardening response under uniaxial loading.

Keywords: Micromechanics, Fiber-reinforced cementitious materials, Fractures, Damage propagation, Anisotropy

1 Introduction

Most well-known solid materials exhibit heterogeneities at different scales and orientations. A representative example is fiber-reinforced cementitious materials, which combine a cement-based matrix with a discrete distribution of fibers to improve their mechanical properties. In addition to fiber inclusions, these materials are also prone to the emergence and propagation of cracks or fractures — regions of small thickness along which the mechanical and physical properties of the material are degraded. Understanding fracture mechanisms and developing techniques for their prevention and mitigation is critical to ensuring the safety and performance of cementitious materials in a wide range of applications. In this context, the embedded fibers play a key role in bridging these fractures, enhancing the post-cracking strength and improving both tensile behavior and fracture toughness.

The assessment of the macroscopic properties of heterogeneous media, such as fiber-reinforced fractured cementitious materials, is a complex task due to their morphological complexity, which makes them one of the major concerns in structural engineering. Homogenization theory provides efficient tools to simplify the mathematical treatment of heterogeneous media and derive their effective macroscopic properties [1]. However, when dealing with such composites, it is essential to incorporate a damage evolution mechanism into the formulation. Damage mechanics offers a rigorous framework by introducing internal variables that control stiffness degradation [2].

This work will address the particular situation of a fiber-reinforced fractured cementitious materials. For that, we must quote the relevant contributions of [3–6], which proposed general micromechanics-based approaches for macroscopic behavior of fiber-reinforced cementitious materials and fractured media. The main contribution of the present work is to combine the micromechanical approach from Guimarães et al. [6] for the macroscopic behavior of fiber-reinforced fractured cementitious materials with macroscopic thermodynamic principles to develop a macroscopic damage model, following the approach proposed by Guimarães et al. [5].

The micromechanical approach is briefly outlined in section 2, followed by the derivation of the homogenized elastic behavior of fiber-reinforced fractured cementitious materials in section 3. Section 4 deals with the macroscopic damage model and its experimental validation. Conclusions and final remarks are provided in section 5.

2 Micromechanics

Let Ω denote the representative elementary volume (REV) of a cementitious matrix Ω^m reinforced by fibers $\Omega^r = \cup_i \Omega_i^r$ and cut by a discrete distribution of microfractures $\omega = \cup_i \omega_i$. The REV is assumed to be statistically representative of the heterogeneous medium and is chosen such that the characteristic size d of the heterogeneities (e.g., fibers and fractures) is supposed to be small enough as compared to the REV dimension ℓ, which in turn is supposed to be sufficiently smaller than the characteristic dimension L of the whole structure. Furthermore, the REV size ℓ must be sufficiently smaller than the wavelength λ of the macroscopic solicitation. The previous scale separation condition may be summarized as $d \ll \ell \ll L$, and $\ell \ll \lambda$. At the scale of REV (microscopic scale), each fiber family Ω_i^r is modeled as a three-dimensional material, and each fracture family is modeled as an interface ω_i, geometrically described by a surface whose orientation is defined by a normal unit vector $\underline{n}_i$, as depicted in Fig. 1.

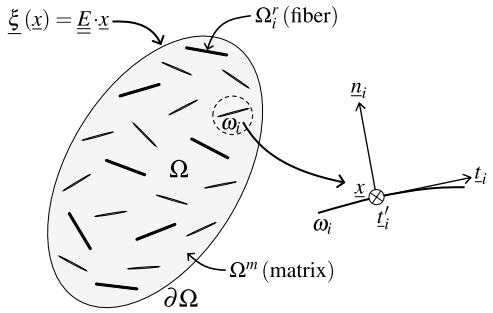


Figure 1. Representative elementary volume and loading mode

The cementitious matrix and the fibers fill the domain $\Omega^m \cup \Omega^r = \Omega \backslash \omega$, where the symbol "\" represents the difference between the REV domain Ω and the fractures ω. Note that strains and stresses within the heterogeneous medium are defined only in the domain $\Omega \backslash \omega$ and not on the whole REV. Throughout the paper, the symbol $\langle \cdot \rangle$ denotes the volume average over the region occupied by the cementitious matrix and fibers:

$$\langle \cdot \rangle = \frac{1}{|\Omega|} \int_{\Omega \backslash \omega} \cdot \, d\Omega. \tag{1}$$

2.1 Hill's Lemma for the fractured media

The loading applied to the REV is defined by a homogeneous strain type boundary conditions

$$\underline{\xi}(\underline{x}) = \underline{\underline{E}} \cdot \underline{x} \quad \forall \underline{x} \in \partial\Omega, \tag{2}$$

where $\underline{\underline{E}}$ denotes the macroscopic strain and $\underline{x}$ is the position vector. The Hill's lemma for the fractured medium, for any statically admissible stress field $\underline{\underline{\sigma}}$ and any kinematically admissible displacement field $\underline{\xi}$ is given by:

$$\left\langle \underline{\underline{\sigma}} \right\rangle : \underline{\underline{E}} = \left\langle \underline{\underline{\sigma}} : \underline{\underline{\varepsilon}} \right\rangle + \frac{1}{|\Omega|} \int_{\omega} \underline{T} \cdot [\![\underline{\xi}]\!] \, dS, \tag{3}$$

in which $\underline{T} = \underline{\underline{\sigma}} \cdot \underline{n}_i$ is the stress vector acting upon the fracture and $[\![\underline{\xi}]\!]$ is the displacement jump observed at the fracture interface [4]. It is noted that $\underline{\underline{\Sigma}} = \left\langle \underline{\underline{\sigma}} \right\rangle$ represents the macroscopic stress equilibrated by the microscopic stress field $\underline{\underline{\sigma}}$ defined in the REV Ω. The strain average rule relating the macroscopic strains to the local strains writes as $\underline{\underline{E}} = \left\langle \underline{\underline{\varepsilon}} \right\rangle + \frac{1}{|\Omega|} \int_{\omega} [\![\underline{\xi}]\!] \overset{s}{\otimes} \underline{n} \; dS$, where the symbol $\overset{s}{\otimes}$ stands for the symmetric part of a dyadic product.

2.2 Homogenization elastic framework

In the context of linear elasticity, stresses $\underline{\underline{\sigma}}$ and strains $\underline{\underline{\varepsilon}}$ fields in the cementitious matrix and fibers are related through the fourth-order stiffness tensors $\mathbb{C}^m$ and $\mathbb{C}_i^r$, respectively. The stress vector $\underline{T}$ is related to the displacement

jump $[\![\underline{\xi}]\!]$ along fractures through the second-order stiffness tensor $\underline{\underline{k}}_i^f$. These relationships are summarized by:

$$\underline{\underline{\sigma}} = \begin{cases} \mathbb{C}^m : \underline{\underline{\varepsilon}} & \text{in } \Omega^m \\ \mathbb{C}_i^r : \underline{\underline{\varepsilon}} & \text{in } \Omega_i^r \end{cases} \quad \text{and} \quad \underline{T} = \underline{\underline{\sigma}} \cdot \underline{n}_i = \underline{\underline{k}}_i^f \cdot [\![\underline{\xi}]\!] \quad \text{along } \omega_i. \tag{4}$$

The loading condition (eq. (2)) combined to the state equations (eq. (4)) constitute the elastic concentration problem, which solution is given by the pair $\left(\underline{\sigma}, \underline{\xi}\right)$. The local strains $\underline{\underline{\varepsilon}}(\underline{x})$ linearly depend on the loading parameter $\underline{\underline{E}}$ through the concept of strain concentration tensor [1]:

$$\underline{\underline{\varepsilon}}(\underline{x}) = \mathbb{A}(\underline{x}) : \underline{\underline{E}} \quad \forall \underline{x} \in \Omega \backslash \omega. \tag{5}$$

The fourth-order tensor $\mathbb{A}$ is the strain concentration tensor, linking the local strains $\underline{\underline{\varepsilon}}(\underline{x})$ in the $\Omega \backslash \omega$ domain to the macroscopic strain $\underline{\underline{E}}$ applied to the REV. In contrast to a continuum framework, where the volume average of strain concentration tensor over the REV is equal to the fourth-order identity tensor, the analysis involving discontinuities leads to $\langle \mathbb{A} \rangle \neq \mathbb{I}$. This discrepancy occurs due to the fraction of macroscopic strain that localizes in the fractures [4]. A classical reasoning in linear elastic homogenization [1] shows that:

$$\underline{\underline{\Sigma}} = \mathbb{C}^{hom} : \underline{\underline{E}} \quad \text{with} \quad \mathbb{C}^{hom} = \langle \mathbb{C} : \mathbb{A} \rangle, \tag{6}$$

where $\mathbb{C}^{hom}$ denotes the macroscopic elastic stiffness tensor. For a multi-phase composite, $\mathbb{C}^{hom}$ takes the form:

$$\mathbb{C}^{hom} = \sum_{p=1}^{n} f^p \mathbb{C}^p : \langle \mathbb{A} \rangle_{\Omega^p}, \tag{7}$$

in which f^p, $\mathbb{C}^p$ and $\langle \mathbb{A} \rangle_{\Omega^p} = \frac{1}{|\Omega^p|} \int_{\Omega^p} \mathbb{A}(\underline{x}) \, dV$ are the volume fraction, the elastic stiffness tensor, and the average strain concentration tensor in the phase p, respectively. Therefore, the determination of $\mathbb{C}^{hom}$ reduces to evaluating $\langle \mathbb{A} \rangle_{\Omega^p}$. For this purposes, fractures will be modeled as 3D spheroidal heterogeneities (rather than 2D interfaces) with an equivalent elastic behavior [4–6]. The following reasoning is developed in the Eshelby's equivalent inclusion theory [7] context, resorting to the Mori-Tanaka scheme [8] to compute $\langle \mathbb{A} \rangle_{\Omega^p}$ and $\mathbb{C}^{hom}$.

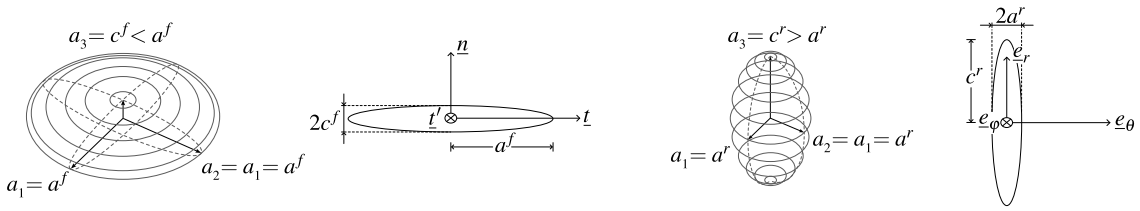
3 Homogenized elastic properties of fiber-reinforced fractured cementitious materials

In this section, the macroscopic stiffness tensor $\mathbb{C}^{hom}$ for fiber-reinforced fractured cementitious materials will be addressed. From a geometrical viewpoint, fractures are modeled as a set of oblate spheroids with an attached orthonormal frame $(\underline{t}, \underline{t}', \underline{n})$. The oblate radius is denoted by a^f, while c^f represents its half-opening. The aspect ratio of such penny-shaped fracture is given by $X^f = c^f / a^f$, which satisfies the condition $X^f \ll 1$. On the other hand, fibers are modeled as a set of prolate spheroids associated with the orthonormal frame $\left(\underline{e}_\theta, \underline{e}_\varphi, \underline{e}_r\right)$. The fiber shape is defined by the aspect ratio $X^r = c^r / a^r$, where c^r and a^r denote the semi-major and semi-minor radii of the prolate spheroid. Figure 2 illustrates the geometrical inclusion properties. In the continuum micromechanics approach employed herein, fractures and fibers are treated as inhomogeneities embedded within the cementitious matrix, and the stiffness tensors of each material phase are assumed to take the following form:

$$\mathbb{C}^m = 3k^m \mathbb{J} + 2\mu^m \mathbb{K}, \;\; \mathbb{C}_i^r = 3k_i^r \mathbb{J} + 2\mu_i^r \mathbb{K}, \;\; \text{and} \;\; \underline{\underline{k}}_i^f = k_{n_i}^f \left(\underline{n}_i \otimes \underline{n}_i\right) + k_{t_i}^f \left(\underline{t}_i \otimes \underline{t}_i + \underline{t}_i' \otimes \underline{t}_i'\right), \tag{8}$$

where k^m and μ^m are the bulk and shear moduli of the cementitious matrix, while k_i^r and μ_i^r correspond to the bulk and shear moduli of the i-th fiber family. The fourth-order projection tensors $\mathbb{J}$ and $\mathbb{K}$ are defined as $\mathbb{J} = \frac{1}{3} \underline{\underline{1}} \otimes \underline{\underline{1}}$ and $\mathbb{K} = \mathbb{I} - \mathbb{J}$. The scalars $k_{n_i}^f$ and $k_{t_i}^f$ denote the normal and shear stiffness of the i-th fracture family, typically obtained from laboratory tests performed on specimens with a single fracture (see [9, 10] for more details).

We consider that the fractures belonging to a given family are defined by the same radius a_i^f and aspect ratio X_i^f. The volume fraction of each fracture family is denoted by $f_i^f = \frac{4}{3} \pi \varepsilon_i^f X_i^f$, where $\varepsilon_i^f = \mathcal{N}_i^f (a_i^f)^3$ is the fracture density parameter, introduced by Budiansky and O'connell [11], and $\mathcal{N}_i^f$ represents the number of fractures per unit volume. Similarly, fibers within a given family share the same properties (a_i^r, X_i^r), and f_i^r denotes the fiber family volume fraction. Given that the total volume fractions sums to one, the matrix volume fraction is $f^m = 1 - f^f - f^r$, where $f^f = \sum_i f_i^f$ and $f^r = \sum_i f_i^r$.



(a) Fracture modeled as oblate spheroid (b) Fiber modeled as prolate spheroid

Figure 2. Ellipsoidal geometries used in the micromechanical modeling of fractures and fibers

Based on interface layer modeling, Maghous et al. [4] introduced the elastic isotropic fourth-order fracture tensor $\mathbb{C}_i^f$ to represent the equivalent behavior of fractured modeled as interfaces:

$$\mathbb{C}_i^f = 3X_i^f a_i^f \left(k_{n_i}^f - \frac{4}{3}k_{t_i}^f\right)\mathbb{J} + 2X_i^f a_i^f k_{t_i}^f \mathbb{K} \text{ with } X_i^f \ll 1. \tag{9}$$

Using a Mori-Tanaka scheme [8], the estimate of tensor $\mathbb{C}^{hom}$ for the fiber-reinforced fractured cementitious material reads:

$$\begin{aligned}\mathbb{C}^{hom} = \lim_{X_1^f,\ldots,X_n^f \to 0} \Bigg\{ &\left[f^m\mathbb{C}^m + \sum_{i=1}^{n} f_i^f \mathbb{C}_i^f : \left(\mathbb{I} + \mathbb{P}_i^{m,f} : \left(\mathbb{C}_i^f - \mathbb{C}^m\right)\right)^{-1} + \sum_{i=1}^{p} f_i^r \mathbb{C}_i^r : \left(\mathbb{I} + \mathbb{P}_i^{m,r} : \left(\mathbb{C}_i^r - \mathbb{C}^m\right)\right)^{-1} \right] : \\ &\left[f^m\mathbb{I} + \sum_{i=1}^{n} f_i^f \left(\mathbb{I} + \mathbb{P}_i^{m,f} : \left(\mathbb{C}_i^f - \mathbb{C}^m\right)\right)^{-1} + \sum_{i=1}^{p} f_i^r \left(\mathbb{I} + \mathbb{P}_i^{m,r} : \left(\mathbb{C}_i^r - \mathbb{C}^m\right)\right)^{-1} \right]^{-1} \Bigg\}\end{aligned} \tag{10}$$

where $\mathbb{P}_i^{m,f}$ and $\mathbb{P}_i^{m,r}$ are the Hill tensors associated with the i-th fracture family (oblate spheroid) and the i-th fiber family (prolate spheroid), respectively. They depend on the aspect ratios of the correspond ellipsoidal inclusions and their orientations. Closed-form solutions of Hill tensors $\mathbb{P}_i^{m,f}$ and $\mathbb{P}_i^{m,r}$ can be found in Handbooks (e.g., [12, 13]). The general estimate of $\mathbb{C}^{hom}$ (eq. (10)) can be particularized for several configurations involving discrete distributions of fractures and fibers (see Guimarães et al. [6], for instance). Particular cases of cracked cementitious materials reinforced by fibers are assessed by taking $\underline{\underline{k}}_i^f = 0$ in the above estimate.

4 Micromechanical damage model

This section presents a macroscopic damage model within the framework of linear elasticity for fiber-reinforced fractured cementitious materials treated as a homogenized medium. The model formulated by Guimarães et al. [5] combines micromechanical results with classical thermodynamic principles, reflecting fracture propagation at the microscopic scale. At the macroscopic scale, the damage is characterized by a single couple of parameters $\left(\varepsilon_i^f, \mathcal{N}_i^f\right)$. However, the present analysis does not address fracture nucleation, and the parameter $\mathcal{N}_i^f$ is assumed to remain constant. Therefore, the damage evolution is only governed by ε_i^f, with $i = 1, \ldots, n$, characterizing a damage vector $\underline{\varepsilon}^f = \left(\varepsilon_1^f, \ldots, \varepsilon_n^f\right)$, while the vector $\underline{\mathcal{N}}^f = \left(\mathcal{N}_1^f, \ldots, \mathcal{N}_n^f\right)$ remains constant for each family. Additionally, the proposed damage model considers that the fiber rupture does not occur during damage evolution (i.e., the volume fraction of resistant fibers remains constant: $\dot{f}^r = 0$). This assumption corresponds to the case of ductile fibers, which can undergo significant deformation without losing their reinforcing capacity.

4.1 Thermodynamic formulation

In isothermal elastic evolutions, the macroscopic volume density of free energy Ψ appears to be a function of three internal variables, namely the macroscopic strain $\underline{\underline{E}}$, and the damage parameters $\underline{\varepsilon}^f$, $\underline{\mathcal{N}}^f$:

$$\Psi = \Psi\left(\underline{\underline{E}}, \underline{\varepsilon}^f, \underline{\mathcal{N}}^f\right) = \frac{1}{2}\underline{\underline{E}} : \mathbb{C}^{nom}\left(\underline{\varepsilon}^f, \underline{\mathcal{N}}^f\right) : \underline{\underline{E}}. \tag{11}$$

The intrinsic dissipation denoted by $\mathcal{D}d\Omega$ is the difference between the work of the external forces provided to the elementary volume and the stored energy. The combination of the first and second principles of thermodynamics yields the Clausius-Duhem inequality [2]:

$$\mathcal{D} = \underline{\underline{\Sigma}} : \dot{\underline{\underline{E}}} - \dot{\Psi} = \left(\underline{\underline{\Sigma}} - \frac{\partial \Psi}{\partial \underline{\underline{E}}} \right) : \dot{\underline{\underline{E}}} - \frac{\partial \Psi}{\partial \underline{\varepsilon}^f} \cdot \dot{\underline{\varepsilon}}^f - \frac{\partial \Psi}{\partial \underline{\mathcal{N}}^f} \cdot \dot{\underline{\mathcal{N}}}^f \geq 0, \tag{12}$$

which holds for any real evolution of the material. Considering the macroscopic state equation $\underline{\underline{\Sigma}} = \partial \Psi / \partial \underline{\underline{E}}$ and restricting the analysis to the absence of nucleation, i.e., $\dot{\underline{\mathcal{N}}}^f = 0$, the dissipation expression reduces to:

$$\mathcal{D} = -\frac{\partial \Psi}{\partial \underline{\varepsilon}^f} \cdot \dot{\underline{\varepsilon}}^f \geq 0. \tag{13}$$

Similarly to Griffith's work [14], the quantity $\underline{\mathcal{F}}\left(\underline{\underline{E}}, \underline{\varepsilon}^f\right) = -\partial \Psi / \partial \underline{\varepsilon}^f$ plays the role of the thermodynamic force responsible for damage evolution:

$$\underline{\mathcal{F}} = -\frac{\partial \Psi}{\partial \underline{\varepsilon}^f} = -\frac{1}{2} \underline{\underline{E}} : \frac{\partial \mathbb{C}^{hom}}{\partial \underline{\varepsilon}^f} : \underline{\underline{E}} = \frac{1}{2} \underline{\underline{\Sigma}} : \frac{\partial \mathbb{S}^{hom}}{\partial \underline{\varepsilon}^f} : \underline{\underline{\Sigma}}, \tag{14}$$

where $\mathbb{S}^{hom}$ is the homogenized compliance tensor that can be obtained by inverting $\mathbb{C}^{hom}$ of eq. (10).

To govern the damage evolution, we need to introduce a surface $H\left(\underline{\mathcal{F}}, \underline{\varepsilon}^f\right) = 0$, which delimits the region where the damage does not propagate in the space of the thermodynamic force $\underline{\mathcal{F}}$. To define this region, Guimarães et al. [5] postulated the damage propagation criterion $H\left(\underline{\mathcal{F}}, \underline{\varepsilon}^f\right) \leq 0$ and derived expressions for the damage multiplier $\dot{\lambda}$ and the damage evolution $\dot{\underline{\varepsilon}}^f$. For simplicity, they adopted two expressions for $H\left(\underline{\mathcal{F}}, \underline{\varepsilon}^f\right) \leq 0$, namely the coupled and the decoupled damage criteria. However, the damage criterion should be chosen based on experimental data. Inspired by Guimarães et al. [5], we adopt the decoupled form due to its mathematical simplicity:

$$H\left(\underline{\mathcal{F}}, \underline{\varepsilon}^f\right) \leq 0 \quad \Leftrightarrow \quad \max_i H_i \leq 0 \quad \text{with} \quad H_i = \mathcal{F}_i - \mathcal{R}_i\left(\varepsilon_i^f\right), \tag{15}$$

where $\mathcal{F}_i$ is the thermodynamic force in according to eq. (14) and the function $\mathcal{R}\left(\varepsilon_i^f\right)$ describes the fracture resistance to damage propagation. It's dependency on ε_i^f confers to the latter the role of a hardening variables. For simplicity, the following form is chosen for $\mathcal{R}_i\left(\varepsilon_i^f\right)$ [15]:

$$\mathcal{R}_i\left(\varepsilon_i^f\right) = k\left(1 + \eta_i \varepsilon_i^f\right), \tag{16}$$

where k describes the damage threshold and η_i accounts for the hardening effect of damage. The propagation condition expressed in eq. (15) implies that:

$$\left\{ \begin{array}{lcl} H < 0 & \Rightarrow & \dot{\underline{\varepsilon}}^f = 0 \\ H = 0 & \Rightarrow & \text{possible } \dot{\underline{\varepsilon}}^f \neq 0 \end{array} \right. \quad \Leftrightarrow \quad \left\{ \begin{array}{lcl} \forall i \; H_i < 0 & \Rightarrow & \dot{\underline{\varepsilon}}^f = 0 \\ \exists i \; H_i = 0 & \Rightarrow & \text{possible } \dot{\underline{\varepsilon}}^f \neq 0 \end{array} \right. \tag{17}$$

In other words, the damage evolution should be calculated individually for the whole i leading condition $H_i = 0$. According to Pavan et al. [16], the evolution of ε_i^f is described through a damage potential $G_i\left(\mathcal{F}_i, \varepsilon_i^f\right)$, which controls the direction of damage evolution:

$$\dot{\varepsilon}_i^f = \dot{\lambda}_i \frac{\partial G}{\partial \mathcal{F}_i}, \tag{18}$$

where the damage multiplier $\dot{\lambda}_i$ must comply with Kuhn Tucker conditions: $\dot{\lambda}_i \geq 0$; $H_i \leq 0$; $\dot{\lambda}_i H_i = 0$. Assuming an associated model $G_i = H_i$ for each i, the damage multiplier $\dot{\lambda}_i$ is obtained from the consistency condition $\dot{H}_i = 0$, and together with eq. (18), it yields the damage evolution law (see [5] for detailed mathematical derivations):

$$\dot{\varepsilon}_i^f = -\frac{\underline{\underline{E}} : \dfrac{\partial \mathbb{C}^{hom}}{\partial \varepsilon_i} : \dot{\underline{\underline{E}}}}{\dfrac{1}{2} \underline{\underline{E}} : \dfrac{\partial^2 \mathbb{C}^{hom}}{\partial (\varepsilon_i^f)^2} : \underline{\underline{E}} + \dfrac{\partial \mathcal{R}_i}{\partial \varepsilon_i^f}} \quad \text{with} \quad \frac{\partial \mathcal{R}_i}{\partial \varepsilon_i^f} = k \eta_i. \tag{19}$$

4.2 Numerical integration of the damage law

This subsection presents the algorithmic aspects to the numerical integration of the proposed model. The evolution of damage parameter $\varepsilon_i^f(t)$ induced by the macroscopic loading will be determined numerically in an incremental manner. Starting from an initial condition $\varepsilon_i^f(t=0) = \varepsilon_{i,0}^f$, the value of k-th time-step, denoted as $\varepsilon_{i,k}^f = \varepsilon_i^f(t=t_k)$, is updated from the previous step $\varepsilon_{i,k-1}^f = \varepsilon_i^f(t=t_{k-1})$ using the following incremental relation:

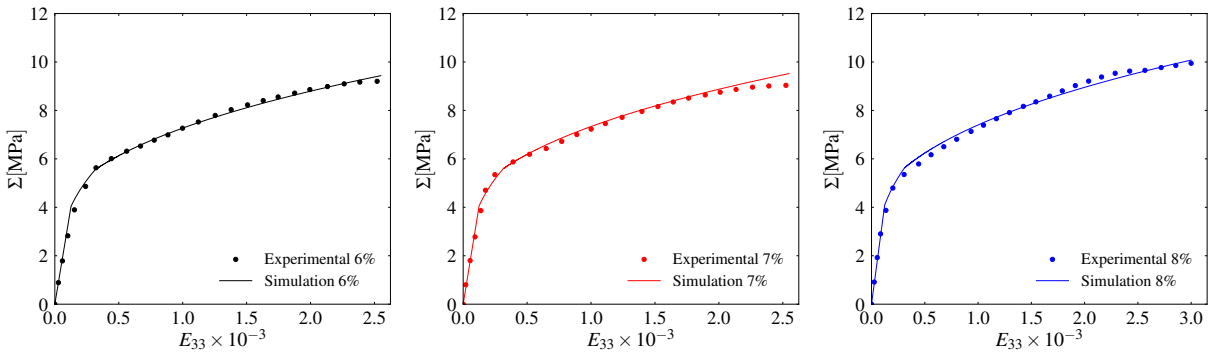
$$\varepsilon_{i,k}^f = \varepsilon_{i,k-1}^f + \dot{\varepsilon}_i^f \Delta t, \tag{20}$$

where Δt is the time discretization and $\dot{\varepsilon}_i^f$ is given by eq. (19). The accuracy of this incremental process is directly correlated to the time discretization $\Delta t(t_k = t_{k-1} + \Delta t)$ and to the scheme used to compute $\dot{\varepsilon}_i^f$. In this work, an explicit integration scheme is adopted, where the damage evolution is evaluated at the previous time step, leading to the approximation $\dot{\varepsilon}_i^f = \dot{\varepsilon}_{i,k-1}^f$ in eq. (20). For further details of numerical procedure, see [5].

4.3 Application of the damage model to an fiber-reinforced cementitious material

In this subsection, we apply the proposed damage model to study the response of randomly distributed steel fiber-reinforced concrete subjected to uniaxial tensile loading, $\underline{\underline{\Sigma}} = \Sigma(t)\underline{e}_3 \otimes \underline{e}_3$. The experimental data were reported by Li and Li [17]: $E^m = 28{,}860$ MPa and $\nu^m = 0.17$ for the concrete matrix; $E^r = 200{,}000$ MPa, $\nu^r = 0.30$, and an aspect ratio of $X^r = 60$ for the steel fibers. The fibers were incorporated into the material at three volume fractions: $f^r \in \{6\%, 7\%, 8\%\}$. In all simulations, we consider an isotropic steel fiber distribution, and concrete discontinuities were modeled as cracks and not as fractures, disregarding the fracture stiffness (i.e., $k_{n_i}^f = k_{t_i}^f = 0$). This simplification has been adopted in order to reduce the parameters in the fitting procedure. A single crack per unit volume was considered, and we set the initial damage parameter to $\varepsilon_{i,0}^f = 0.01$. As a preliminary approximation to the experimental data, nine crack families were adopted to reproduce an isotropic distribution and capture damage induced anisotropy (the spatial crack orientations are found in Appendix B of Guimarães et al. [5]). The initial damage parameter was uniformly distributed among the crack families.

The only parameters that remain to be determined are k and η_i that appear in the expression of the damage criterion. These parameters are taken constant, and the identification procedure consists in calibrating the model parameters k and η_i from the experimental tensile test performed on concrete matrix reinforced by $f^r = 6\%$ of steel fibers. The calibration has been achieved resorting to an appropriate least square minimization procedure, and the numerical values obtained are: $k = 1.32 \times 10^{-3}$ MJ m^{-3} and $\eta_i = 5.84$. The validation of the model calibrated according to the procedure described above is performed by comparing the simulations for a concrete matrix containing a volume fractions of 6%, 7% and 8% of steel fibers. Figure 3 shows the overall stress-strain response in tensile tests for $f^r = 6\%$, $f^r = 7\%$, and $f^r = 8\%$. As illustrated, the model predictions can relevantly reproduce the main features of fiber-reinforced concrete behavior under uniaxial tensile loading. The excellent fit obtained for the simulated response at $f^r = 6\%$ confirms the calibration procedure accuracy. The results predicted for the simulation at $f^r = 7\%$ and $f^r = 8\%$ also show good agreement with experimental data; this indicates the good predictive capabilities of the proposed micromechanical damage model. It has been observed from the numerical simulations that nine crack families can reproduce the damage induced anisotropy phenomenon.



(a) 6% steel fiber content (b) 7% steel fiber content (c) 8% steel fiber content

Figure 3. Comparison of the tensile tests of randomly steel fiber-reinforced concrete

5 Conclusions

In the present study we investigate and evaluate the effective elastic properties of fiber-reinforced fractured cementitious materials. The macroscopic elastic properties of these composite materials have been performed in the framework of Eshelby's equivalent inclusion theory, employing the Mori-Tanaka scheme to estimate the $\mathbb{C}^{hom}$ tensor. A damage model for fiber-reinforced fractured cementitious materials is introduced, following the approach of Guimarães et al. [5], which combines micromechanical results with classical thermodynamics arguments. A particular expression is adopted for the damage propagation criterion, and the numerical integration of the damage law is presented. Finally, a validation of the proposed micromechanical damage model through a comparison with experimental results reported by Li and Li [17] on a steel fiber-reinforced concrete is presented. The numerical predictions of the damage model are in good agreement with the available experimental data.

Acknowledgements. The authors are grateful for the financial support provided by CAPES and CNPq.

Authorship statement. The authors hereby confirm that they are the sole liable persons responsible for the authorship of this work, and that all material that has been herein included as part of the present paper is either the property (and authorship) of the authors, or has the permission of the owners to be included here.

References

[1] A. Zaoui. Continuum micromechanics: survey. *Journal of Engineering Mechanics*, vol. 128, n. 8, pp. 808–816, 2002.

[2] J. Lemaitre and J. L. Chaboche. *Mechanics of solid materials*. Cambridge university press, 1994.

[3] V. P. Dutra, S. Maghous, A. Campos Filho, and A. Pacheco. A micromechanical approach to elastic and viscoelastic properties of fiber reinforced concrete. *Cement and concrete research*, vol. 40, n. 3, pp. 460–472, 2010.

[4] S. Maghous, L. Dormieux, D. Kondo, and J. Shao. Micromechanics approach to poroelastic behavior of a jointed rock. *International Journal for Numerical and Analytical Methods in Geomechanics*, vol. 37, n. 2, pp. 111–129, 2013.

[5] M. B. Guimarães, de C. B. Aguiar, and S. Maghous. Upscaling modeling of effective elastic properties and anisotropic damage propagation in fractured materials regarded as homogenized media. *Journal of the Brazilian Society of Mechanical Sciences and Engineering*, vol. 46, n. 1, pp. 47, 2024a.

[6] M. B. Guimarães, de C. B. Aguiar, and S. Maghous. A micromechanical approach to effective elastic properties of fiber-reinforced fractured cementitious materials. In *Ibero-Latin American Congress on Computational Methods in Engineering (CILAMCE)*, 2024b.

[7] J. D. Eshelby. The determination of the elastic field of an ellipsoidal inclusion, and related problems. *Proceedings of the royal society of London. Series A. Mathematical and physical sciences*, vol. 241, n. 1226, pp. 376–396, 1957.

[8] T. Mori and K. Tanaka. Average stress in matrix and average elastic energy of materials with misfitting inclusions. *Acta metallurgica*, vol. 21, n. 5, pp. 571–574, 1973.

[9] R. E. Goodman. Methods of geological engineering in discontinuous rocks. *(No Title)*, vol. 13, 1976.

[10] S. C. Bandis, A. C. Lumsden, and N. R. Barton. Fundamentals of rock joint deformation. In *International Journal of Rock Mechanics and Mining Sciences & Geomechanics Abstracts*, volume 20, pp. 249–268. Elsevier, 1983.

[11] B. Budiansky and R. J. O'connell. Elastic moduli of a cracked solid. *International journal of Solids and structures*, vol. 12, n. 2, pp. 81–97, 1976.

[12] T. Mura. *Mechanics of Defects in Solids*. Martinus Nijhoff, 2 edition, 1987.

[13] S. Nemat-Nasser and M. Hori. *Micromechanics: Overall Properties of Heterogeneous Materials*, volume 37. Elsevier Ltd, 1 edition, 1993.

[14] A. A. Griffith. The phenomena of rupture and flow in solids. *Philosophical transactions of the royal society of london. Series A, containing papers of a mathematical or physical character*, vol. 221, n. 582-593, pp. 163–198, 1921.

[15] V. Pensee and D. Kondo. Micromechanics of anisotropic brittle damage: comparative analysis between a stress based and a strain based formulation. *Mechanics of materials*, vol. 35, n. 8, pp. 747–761, 2003.

[16] R. C. Pavan, G. J. Creus, and S. Maghous. A simplified approach to continuous damage of composite materials and micromechanical analysis. *Composite Structures*, vol. 91, n. 1, pp. 84–94, 2009.

[17] F. Li and Z. Li. Continuum damage mechanics based modeling of fiber reinforced concrete in tension. *International journal of solids and structures*, vol. 38, n. 5, pp. 777–793, 2001.